유연인쇄전자학술지, 2022년 6월, 제1권 제1호, pp. 111-118
Journal of Flexible & Printed Electronics, June 2022, Vol. 1, Issue 1, pp. 111-118
Received 2022-07-21, Revised 2022-08-16, Accepted 2022-08-23
https://doi.org/10.56767/jfpe.2022.1.1.111
eISSN: 2951-2174

RESEARCH

Effect of Bias Stress in Inkjet-Printed Polymer Thin-Film Transistors: Generation and Annihilation of Subgap Density of States

Jiyoul Lee[1*], Jaeman Jang[2], Jong Won Chung[3], Bang-Lin Lee[3], Dae Hwan Kim[2*]

[1]Department of Smart Green Technology Engineering and Department of Nanotechnology Engineering, Pukyong National University, Busan, Korea

[2]School of Electrical Engineering, Kookmin University, Seoul, Korea

[3]Material Research Center, Samsung Advanced Institute of Technology, Suwon, Korea

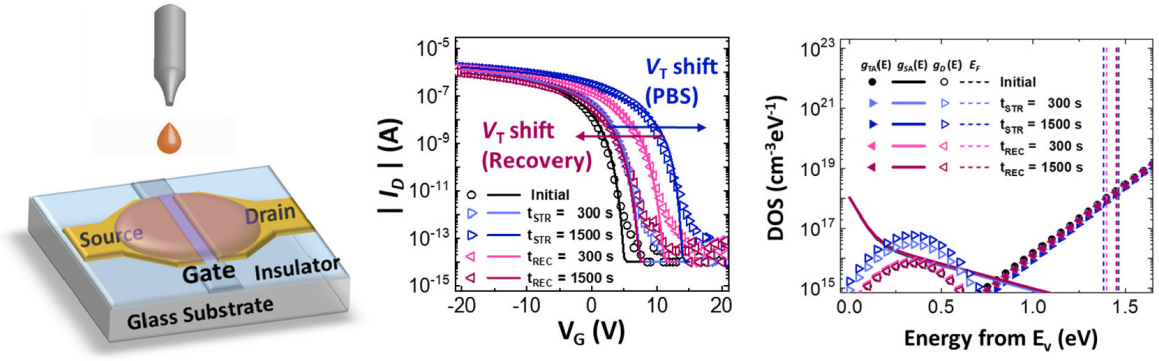

ABSTRACT

Here, we report investigations of the effects of bias stress on the density of states (DOS) in polymer thin-film transistors (PTFTs). As the active channel layer, these PTFTs employed an inkjet-printed semiconducting film of P8T2Z-C12 [poly (tetryldodecyloctathiophene-alt-didodecyl bithiazole)]. In positive bias stress tests, the threshold voltage (V_T) of the inkjet-printed PTFT shifted in the positive direction. However, this shift was largely recovered when the PTFT was released from the bias stress. We analyzed the effect of the bias stress manifested by the V_T shift using the full energy range of the subgap DOS versus the duration of the bias stress, which we obtained by applying various DOS extraction techniques.

Key Words: Polymer semiconductor, Bias stress effect, Density of states (DOS), Inkjet printing, Thin-film transistor

*Correspondence: jiyoul_lee@pknu.ac.kr, drlife@kookmin.ac.kr

1. INTRODUCTION

Organic printed electronic devices, which are made by directly printing functional organic semiconductor inks onto flexible substrates, have been investigated extensively for next-generation flexible electronics be-

cause of their mechanical flexibility and the potentially low cost of manufacturing them using graphic-art printing techniques [1-6]. Among the various printed electronic devices based on π-conjugated polymer semiconducting materials, polymer thin-film transistors (PTFTs) have shown considerable potential for widespread use as crucial building blocks for logic, arithmetic, and memory circuits for future electronic systems [2-4]. However, despite their considerable potential, the electrical instability of PTFTs caused by bias stress remains a major problem that needs to be addressed and solved to enable further developments of PTFT technology [3,7-9]. Here, we report an investigation of the effects of bias stress on the density of states (DOS) in PTFTs with electron donor-acceptor type conjugated copolymers of poly(tetryldodecyloctathiophene-*alt*-didodecylbithiazole)-P8T2Z-C12[the chemical structure is shown in Fig. 1(a)]-which were inkjet-printed to form an active channel layer [10]. The threshold voltage (V_T) of the inkjet-printed PTFT shifted in the positive direction when the gate of the PTFT was subjected to positive bias stress (PBS), whereas it shifted in the opposite (negative) direction when the gate bias (V_G) was removed. We analyzed the effect of the bias stress manifested by the V_T shift by monitoring the device parameters and the DOS extracted from a combination of generation-recombination current spectroscopy, multi-frequency capacitance-voltage spectroscopy [11,12], and current-voltage (I-V) modeling [13-15]. The extracted subgap DOS revealed that the subgap states of the acceptors in the active channel strongly affect the V_T shift of the inkjet-printed PTFTs during operation. We also dis cuss the physical mechanism of the electrical instability induced by bias stress

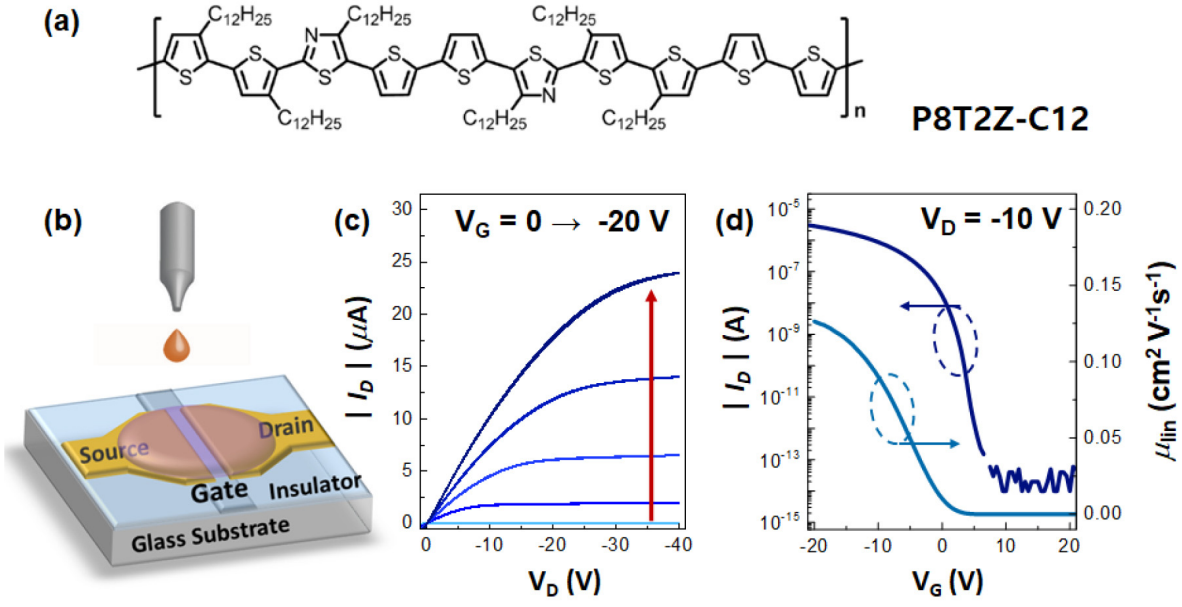

Fig. 1. (a) Chemical structure of the P8T2Z-C12 semiconducting copolymer, (b) schematic of the coplanar PTFT fabricated via inkjet printing, (c) output curves of the inkjet-printed P8T2Z-C12 PTFT, (d) transfer curve and gate-voltage-dependent mobility plots of the PTFT at V_D=-10 V.

in terms of the subgap DOS.

2. METHODS

We measured the electrical properties of P8T2Z-C12-based inkjet-printed PTFTs using a bottom-gate, coplanar, structured device without any passivation to accelerate the electrical degradation, as shown in Fig. 1(b). Except for the passivation process, we fabricated the inkjet-printed PTFT as described previously [3]. We performed the electrical measurements under ambient conditions (relative humidity 30%) using an Agilent 4284A LCR meter and a 4156C semiconductor analyzer.

3. RESULTS AND DISCUSSION

Fig. 1(c) and Fig. 1(d) show representative output and transfer curves, respectively, of the inkjet-printed P8T2Z-C12 PTFT. The output characteristics show reasonable saturation with low hysteresis. As the drain bias (V_D) increases, the output current, I_D, becomes larger than ~25 μA at V_D=−40 V and V_G=−20 V. The transfer characteristics exhibit p-type behavior, with on/off ratios exceeding ~107. The curves of the mobilities with respect to V_G show that the mobilities in the linear region ($V_D \leq -10$ V) increase gradually with V_G and reach 0.13 $cm^2V^{-1}s^{-1}$ at V_G=−20 V.

Fig. 2(a) and Fig. 2(b) show semilogarithmic-scale transfer curves at V_D=−4 V and the corresponding generation−recombination (I_{G-R}) currents as a function of V_G for the inkjet-printed PTFT during PBS at V_G=20 V and V_D=−10 V together with the recovery obtained by releasing the V_G from the PTFT. The symbols in the graph are from the electrical measurements, and the lines are from calculations based on an I−V model [13-15]. As shown in Fig. 2(c), when the PTFT is subject to PBS at V_G=20 V and V_D=−10 V, V_T moves toward more positive values. This means that charge carriers are trapped either in the P8T2Z-C12 polymer layer or at the interface during operation, which con-

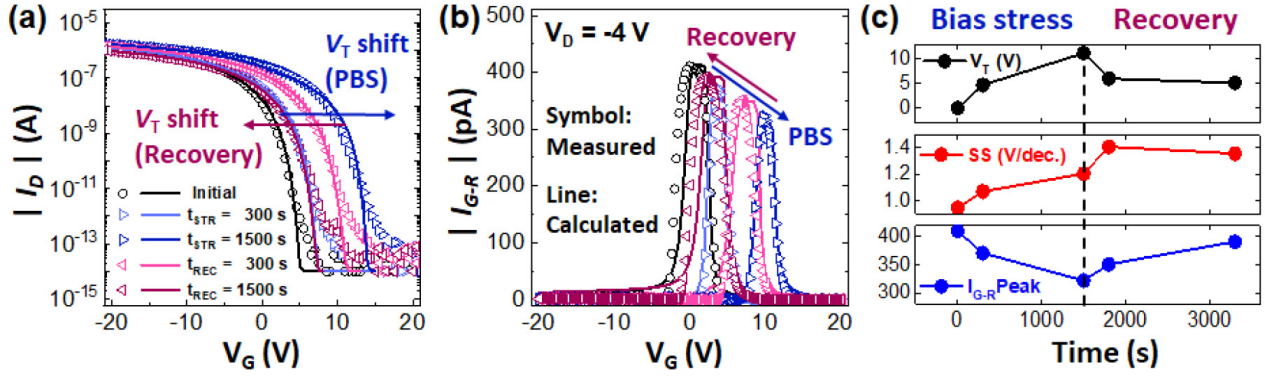

Fig. 2. (a) V_T shifts during PBS and during the recovery process of the P8T2Z-C12 TFT in semilogarithmic-scale transfer curves at V_D=−4 V, (b) the corresponding generation–recombination (I_{G-R}) currents as a function of V_G during PBS and during the recovery process. The symbols are from electrical measurements and the lines are from modeling, (c) extracted electrical parameters from the stress-induced I–V characteristics of the inkjet-printed PTFTs.

sequently shields the gate potential, thereby inducing the V_T shift. The trapping of negative electrons results in the positive shift of V_T. However, V_T recovered (i.e., moved in the negative direction) as the recovery time increased. In addition, the subthreshold swing (S.S.) increased as the duration of the bias stress increased, and it then decreased slightly with increasing recovery time.

The dependence of the changes in these characteristics of the inkjet-printed PTFT upon the duration of the PBS and of the recovery process can be analyzed quantitatively through a physical model based on the full-range DOS. To investigate the effects of bias stress in the PTFTs, we therefore obtained the profiles of the full-range DOS by applying various extraction techniques.

We modeled the DOS function [$g(E)$] in the bandgap of the P8T2Z-C12 polymer channel as a combination of a donor-like DOS [$g_D(E)$], which includes donor-like tail states [$g_{TD}(E)$] and donor-like deep states [$g_{DD}(E)$] near the valence band (E_V), together with shallow acceptor states [$g_{SA}(E)$] and acceptor-like DOS [$g_{TA}(E)$] near the conduction band (E_C). We express this model in terms of the following equations [13],[16]:

$$g_D(E) = g_{TD}(E) + g_{DD}(E) = N_{TD} \times \exp\left(\frac{E_V - E}{kT_{TD}}\right) + N_{DD} \times \exp\left(\frac{E_V - E}{kT_{DD}}\right) \quad (1)$$

$$g_A(E) = g_{SA}(E) + g_{TA}(E) = N_{SA} \times \exp\left[-\left(\frac{E_{SA} - E}{kT_{SA}}\right)^2\right] + N_{TA} \times \exp\left(\frac{E - E_C}{kT_{TA}}\right) \quad (2)$$

where N_{TD}, kT_{TD}, N_{DD}, and kT_{DD} are, respectively, the density of donor-like tail states at $E=E_V$, the characteristic slope of the donor-like tail states, the density of donor-like deep states at $E=E_V$, and the characteristic slope of the donor-like deep states. Similarly, we defined N_{SA}, kT_{SA}, E_{SA}, N_{TA}, and kT_{TA}, respectively, as the peak density of the shallow acceptor states, the characteristic slope of the shallow acceptor states, the position of the peak density of the shallow acceptor states, the density of the acceptor-like tail states at $E=E_C$, and the characteristic slope of the acceptor-like tail states.

Fig. 3 shows the evolution of the full-range DOS function $g(E)$ during the PBS and the recovery process. We note that there is little change in $g_D(E)$ and only a slight change in $g_{TA}(E)$ as the duration of the PBS and the recovery time increase, whereas $g_{SA}(E)$ increases with increasing PBS duration and then decreases with increasing recovery time. Furthermore, the position of the Fermi level (E_F) gradually shifts closer to E_V over time during PBS, leading to a positive shift in V_T, and upon recovery the position of EF

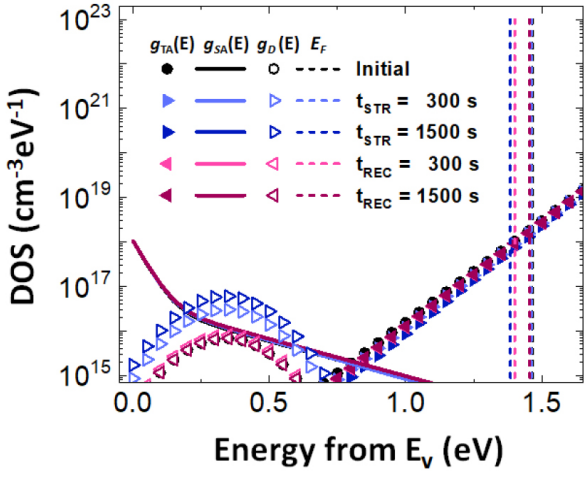

Fig. 3. Evolution of the full-range DOS in the active channel layer of the inkjet-printed P8T2Z-C12 during PBS and the recovery process.

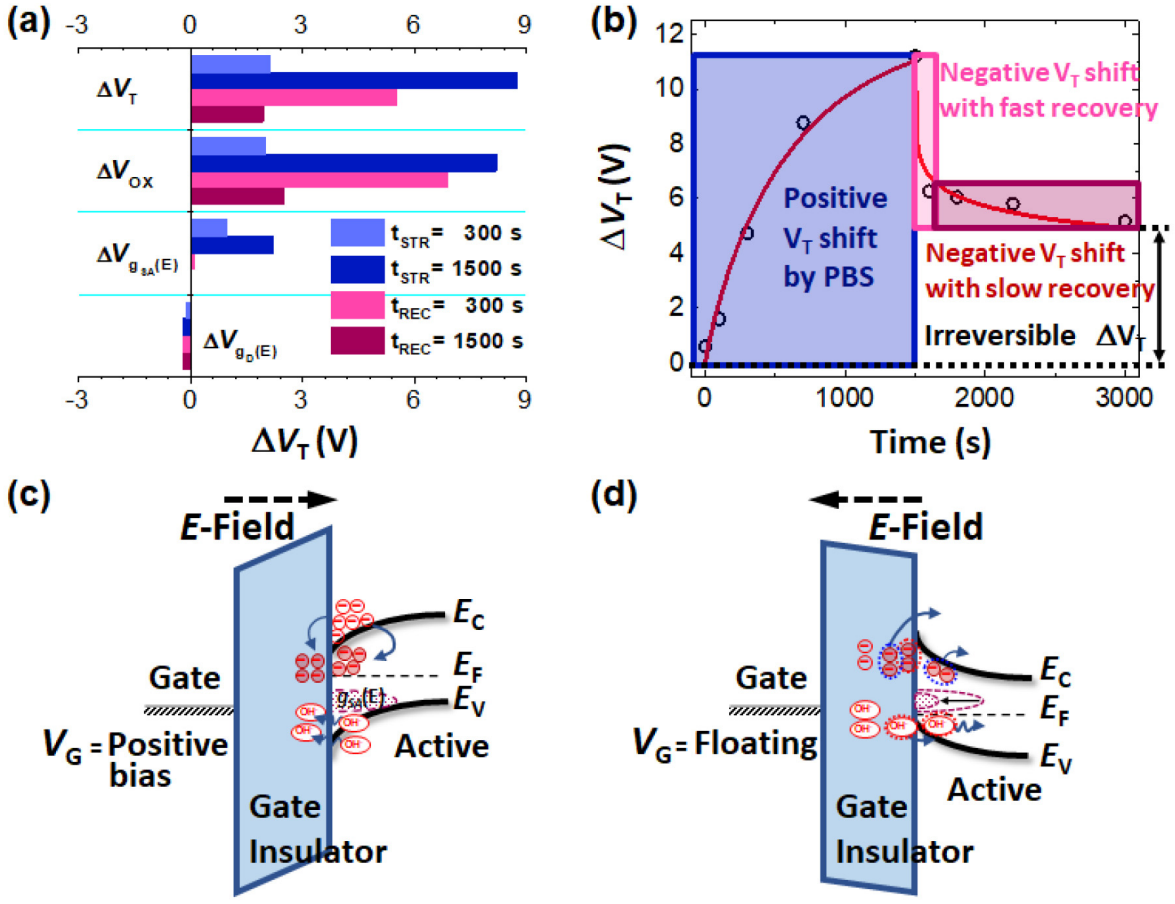

Fig. 4. (a) Dependence of the extracted parameter-dependent portion of ΔV_T on the duration of the PBS and on the recovery time, (b) the changes in ΔV_T as a function of time in the PTFT. The curves are fits using stretched exponential functions, and the symbols are the measured data. The physical mechanisms of the effect of bias stress are represented schematically as energy-band diagrams for (c) PBS and (d) the recovery process.

moves away from E_V, which results in a negative shift in V_T.

Fig. 4(a) shows the portions of the total V_T occupied by each parameter extracted from the I-V modeling and the DOS profile to visualize the effect of each parameter on V_T. The quantity ΔV_{OX} corresponds to the interaction between the charge carriers and the subgap states within the gate insulator. The quantities $\Delta V_{GSA(E)}$ and $\Delta V_{gD(E)}$ are associated with the interactions with the electron-acceptor states and the hole-donor states, respectively, within the active layer. As shown in Fig. 4(a), ΔV_{OX} and $\Delta V_{GSA(E)}$ mainly affect the shifts of V_T during the PBS and the recovery time. However, the effect of $\Delta V_{gD(E)}$, which corresponds to the interaction with hole-donor states, is negligible. Fig. 4(b) shows the changes in ΔV_T as a function of time in the ink-jet-printed PTFT, which was first stressed with V_G= −20 V and V_D=−1 V for 1,500 s, after which the stress was removed. We monitored the changes in ΔV_T by collecting transfer characteristics over the range from

V_G=20 V to −20 V, with V_D=−10 V, at time intervals determined more frequently than in Fig. 2(c). As the duration of the PBS increases, the V_T of the PTFT shifts in the positive direction. At the beginning of the recovery process, V_T first shifts rapidly in the negative direction, but the shift gradually slows down and eventually remains at an irreversible point with increasing recovery time. We fitted ΔV_T for the PBS and recovery process to the respective functions $\Delta V_T(t)=\Delta V_0$ $\{1 - exp [-(t/\tau)^{\beta}]\}$ and $\Delta V_T(t)=\Delta V_{max}$ exp $[-(t/\tau)^{\beta}]$ [17,18]. Here, $\Delta V_0=V_G-V_T^0$, where V_T^0 is the initial threshold voltage, ΔV_{max} is the value of ΔV_T right before the recovery begins, β is the dispersion parameter, and τ is the charge trapping/ detrapping time constant. The fitted values of β and τ are 0.88 and 631 s for PBS and 0.17 and 2,990 s for the recovery process, respectively.

Based on these observations, the physical mechanisms for the changes in the PTFT ΔV_T during the PBS and the recovery process can be expressed schematically as shown in Fig. 4(c) and Fig. 4(d), respectively. First, the positive direction shifts of ΔV_T observed in the PTFT under PBS conditions can be explained by four processes: (i) Electrons are induced at the interface between the insulator and the channel by the positive bias applied to the gate, and most of the induced electrons are injected into the insulator by the electric field and are drawn toward the active layer. (ii) Some of the induced electrons at the interface diffuse to and are trapped in the shallow states near the E_C. (iii) Some anions (OH^-), which decompose from the moisture (H_2O) in the air, are absorbed by the polymer layer and are attracted by the positive V_G, resulting in the generation of defect states [$g_{SA}(E)$] near E_V. (iv) Some OH^- ions migrate to the insulator under the influence of the electric field. Conversely, the recovery of ΔV_T caused by releasing the V_G applied to the PTFT is divided into a fast recovery step and a slow recovery step, each of which can be described as two sequential processes: (v) Electrons trapped in the shallow trapping states near EC are immediately detrapped by the electric field applied to the insulator by the floating gate. (vi) When the PBS is removed, most of the OH^- ions that had been attracted to the $g_{SA}(E)$ within the active layer are pushed away from the interface and migrate to the back channel. During this process, the $g_{SA}(E)$ generated by the OH− ions are annihilated as those ions move away. (vii) Most of the OH^- ions trapped inside the insulator by PBS gradually out-diffuse toward the channel through the insulator/active interface. (viii) Some trapped OH^- ions in the insulator remain even after the PBS is removed, leading to the irreversible component of ΔV_T. In addition, some OH^- ions that migrated to the polymer film also can react with the conjugated polymer chain and induce bipolaron states [19].

4. CONCLUSION

We have investigated the effects of bias stress in an inkjet-printed P8T2Z-C12 PTFT in terms of the subgap DOS. Under PBS conditions, the V_T of the PTFT shifts in the positive direction while generating defect states in the subgap DOS of the active semiconducting polymer layers. However, this shift in V_T is mostly recovered when the PBS is removed. We also confirmed experimentally that the defect states in the subgap DOS annihilated during the recovery process.

ABBREVIATIONS

PTFTs: Polymer thin-film transistors
DOS: Density of states
PBS: Positive bias stres

ACKNOWLEDGEMENTS

Author Contributions

JL, JJ, and DHK were involved in experiments, analysis, and discussion. JWC, and B-LL prepare and synthesize the materials. JL, and DHK drafted the manuscript. All authors read and approved the final manuscript.

Funding

This work was supported by the Basic Science Research Program through the National Research Foundation of Korea (NRF) funded by the Ministry of Science, ICT & Future Planning Korean Government, under Grant Nos. (2016R1A5A1012966, 2020R1A2B5B01001979 and 2021R1A2C1007212).

Declarations of competing interests

The authors declare that they have no competing interests.

REFERENCES

[1] Ariasa, A. C.; Ready, S. E.; Lujan, R.; Wong, W. S.; Paul, K. E.; Salleo, A.; Chabinyc, M. L.; Apte, R.; Street, R. A. All Jet-Printed Polymer Thin-Film Transistor Active-Matrix Backplanes. Appl. Phys. Lett. 2004, 85, 3304.

[2] Sirringhaus, H. Materials and Applications for Solution-Processed Organic Field-Effect Transistors. Proc. IEEE, 2009, 97, 1570.

[3] Lee, J.; Kim, D. H.; Kim, J. Y.; Yoo, B.; Park, J. I.; Chung, J. W.; Lee, B. L.; Jung, J. Y.; Park, J. S.; Koo, B.; Im, S.; Kim, J. W.; Song, B.; Jung, M. H.; Jang, J. E.; Jin, Y. W.; Lee, S. Y. Reliable and Uniform Thin-Film Transistor Arrays Based on Inkjet-Printed Polymer Semiconductors for Full Color Reflective Displays. Adv. Mater. 2013, 25, 5886.

[4] Schwartz, D. E.; Ng,T. N. Comparison of Static and Dynamic Printed Organic Shift Registers. IEEE Electron Device Lett. 2013, 34, 271.

[5] Kwon, J.; Takeda, Y.; Shiwaku, R.; Tokito, S.; Cho, K.; Jung, S Three-Dimensional Monolithic Integration in Flexible Printed Organic Transistors. Nat. Commun. 2019, 10, 54.

[6] Baeg, K. J.; Lee, J. Flexible Electronic Systems on Plastic Substrates and Textiles for Smart Wearable Technologies, Adv. Mater. Tech. 2020, 5, 2000071.

[7] Sirringhaus, H. Reliability of Organic Field-Effect Transistors. Adv. Mater. 2009, 21, 3859.

[8] Park, S.; Kim, S. H.; Choi, H. H.; Kang. B.; Cho, K. Recent Advances in the Bias Stress Stability of Organic Transistors. Adv. Funct. Mater. 2019, 30, 1904590.

[9] Iqbal, H. F.; Waldrip, M.; Chen, H.; McCulloch, I.; Jurchescu, O. D. Elucidating the Role of Water-Related Traps in the Operation of Polymer Field-Effect Transistors. Adv. Electron. Mater. 2021, 7, 2100393.

[10] Lee J.; Chung, J. W.; Kim, D. H.; Lee, B. L.; Park, J. I.; Lee, S.; Häusermann, R.; Batlogg, B.; Lee, S. S.; Choi, I.; Kim, I. W.; Kang, M. S. Thin

Films of Highly Planar Semiconductor Polymers Exhibiting Band-Like Transport at Room Temperature. J. Am. Chem. Soc. 2015, 137, 7990.

[11] Bae, M.; Kim, Y.; Kim, S.; Kim, D. M.; Kim, D. H. Extraction of Subgap Donor States in a-IGZO TFTs by Generation-Recombination Current Spectroscopy. IEEE Electron Device Lett, 2011, 32, 1248.

[12] Lee, S.; Park, S.; Kim, S.; Jeon, Y.; Jeon, K.; Park, J. H.; Park, J.; Song, I.; Kim, C. J.; Park, Y.; Kim, D. M.; Kim, D. H. Extraction of Subgap Density of States in Amorphous Ingazno Thin-Film Transistors by Using Multifrequency Capacitance-Voltage Characteristics. IEEE Electron Device Lett., 2011, 31, 231.

[13] Jang, J.; Kim, J.; Bae, M.; Lee, J.; Kim, D. M.; Kim, D. H.; Lee, J.; Lee, B. L.; Koo, B.; Jin, Y. W. Extraction of the Sub-Bandgap Density-of-States in Polymer Thin-Film Transistors with the Multi-Frequency Capacitance-Voltage Spectroscopy. Appl. Phys. Lett. 2012, 100, 133506.

[14] Jeon, Y. W.; Kim, S.; Lee, S.; Kim, D. M.; Kim, D. H.; Park, J.; Kim, C. J.; Song, I.; Park, Y.; Chung, U. I.; Lee, J. H.; Ahn, B. D.; Park, S. Y.; Park, J. H.; Kim, J. H. Subgap Density-of-States-Based Amorphous Oxide Thin Film Transistor Simulator (DeAOTS). IEEE Trans. Elect. DEV. 2010, 57, 2988.

[15] ATLAS Device Simulation Software User's Manual (Silvaco, Santa Clara, CA, 2005).

[16] Oberhoff, D.; Pernstich, K. P.; Gundlach, D. J.; Batlogg, B. Arbitrary Density of States in an Organic Thin Film Field-Effect Transistor Model and Application to Pentacene Devices. IEEE Tran. Electron. Dev. 2007, 54, 17.

[17] Lee, J.; Kim, D. H.; Lee, B. L.; Park, J. I.; Yoo, B.; Kim, J. Y.; Moon, H.; Koo, B.; Jin, Y. W.; Lee, S. Characterization of Bias Stress induced Electrical Instability in Liquid-Crystalline Semiconducting Polymer Thin-Film Transistors. J. Appl. Phys. 2011, 110, 084511.

[18] Tang, W.; Zhao, J.; Huang, Y.; Ding, L.; Li, Q.; Li, J.; You, P.; Yan, F.; Guo, X. Bias Stress Stability Improvement in Solution-Processed Low-Voltage Organic Field-Effect Transistors Using Relaxor Ferroelectric Polymer Gate Dielectric, IEEE Electron Device Lett., 2017, 38, 748.

[19] Street, R. A.; Salleo, A.; Chabinyc, M. L. Bipolaron Mechanism for Bias-Stress Effects in Polymer Transistors. Phys. Rev. B, 2003, 68, 085316.